Protist, Vol. 170, 125683, December 2019
http://www.elsevier.de/protis
Published online date 21 October 2019

Protist

ORIGINAL PAPER

Novel Lineages of Oxymonad Flagellates from the Termite *Porotermes adamsoni* (Stolotermitidae): the Genera *Oxynympha* and *Termitimonas*

Renate Radek[a,1], Katja Meuser[b], Samet Altinay[a], Nathan Lo[c], and Andreas Brune[b,1]

[a]Evolutionary Biology, Institute for Biology/Zoology, Freie Universität Berlin, 14195 Berlin, Germany
[b]Research Group Insect Gut Microbiology and Symbiosis, Max Planck Institute for Terrestrial Microbiology, 35043 Marburg, Germany
[c]School of Life and Environmental Sciences, The University of Sydney, Sydney, NSW 2006, Australia

Submitted January 21, 2019; Accepted October 9, 2019
Monitoring Editor: Alastair Simpson

The symbiotic gut flagellates of lower termites form host-specific consortia composed of Parabasalia and Oxymonadida. The analysis of their coevolution with termites is hampered by a lack of information, particularly on the flagellates colonizing the basal host lineages. To date, there are no reports on the presence of oxymonads in termites of the family Stolotermitidae. We discovered three novel, deep-branching lineages of oxymonads in a member of this family, the damp-wood termite *Porotermes adamsoni*. One tiny species (6–10 μm), *Termitimonas travisi*, morphologically resembles members of the genus *Monocercomonoides,* but its SSU rRNA genes are highly dissimilar to recently published sequences of Polymastigidae from cockroaches and vertebrates. A second small species (9–13 μm), *Oxynympha loricata,* has a slight phylogenetic affinity to members of the Saccinobaculidae, which are found exclusively in wood-feeding cockroaches of the genus *Cryptocercus*, the closest relatives of termites, but shows a combination of morphological features that is unprecedented in any oxymonad family. The third, very rare species is larger and possesses a contractile axostyle; it represents a phylogenetic sister group to the Oxymonadidae. These findings significantly advance our understanding of the diversity of oxymonads in termite guts and the evolutionary history of symbiotic digestion.

Key words: Evolution; flagellate; molecular phylogeny; Oxymonadida; symbiont; ultrastructure.

Introduction

Symbiotic flagellates in the hindgut of lower termites and wood-feeding cockroaches (genus *Cryptocercus*) are responsible for the digestion of lignocellulose (Brune and Ohkuma 2011; Brune

[1]Corresponding authors;
e-mails renate.radek@fu-berlin.de (R. Radek),
brune@mpi-marburg.mpg.de (A. Brune).

https://doi.org/10.1016/j.protis.2019.125683

2014). Proctodeal trophallaxis not only provides all colony members with the same set of microbial symbionts but also ensures their vertical transmission to the next generation, which favors coevolution of the symbionts with their respective host (Brune and Dietrich 2015). Therefore, termites generally possess host-specific flagellate communities, and members of the same host families typically share closely related symbionts (e.g., Honigberg 1970; Kitade 2004; Tai et al. 2015; Yamin 1979).

The symbiotic gut flagellates of lower termites belong exclusively to the phylum Parabasalia and the Oxymonadida (phylum Preaxostyla), which have been classified as members of the supergroup Excavata (Adl et al. 2019). Oxymonads are anaerobic protists that lack mitochondria and differ from parabasalids by the absence of hydrogenosomes, a discrete dictyosomal Golgi apparatus, and other cell organelles (Brugerolle 1991; Burki 2016). They have a unique cytoskeleton composed of two (or a multiple of two) pairs of basal bodies that are connected by a preaxostyle and give rise to several root structures and a stronger microtubular rod (axostyle) (Brugerolle and Lee 2000; Brugerolle and Radek 2006). Various attempts have been made to homologize basic cytoskeletal elements of Metamonada with the derived structures present in oxymonads (Hampl 2016; Radek 1994; Simpson et al. 2002; Yubuki and Leander 2013, Yubuki et al. 2016); here, we follow largely the terminology of Simpson et al. (2002) to avoid terminological confusion.

The phylogenetic relationships among the oxymonads are only poorly resolved (Radek et al. 2014). Molecular data are scarce, and SSU rRNA gene sequences of only a limited number of species have been reported (Heiss and Keeling 2006; Moriya et al. 1998, 2003; Radek et al. 2014; Stingl and Brune 2003). Some family level taxa are represented only by a few phylotypes. In most lower termites, the presence of oxymonads has not been investigated or is based exclusively on microscopy observations, which are clearly biased towards the larger species (Yamin 1979). In some of the most basal termite lineages, such as members of the family Stolotermitidae, oxymonads have not been reported at all.

The Stolotermitidae comprise the genera *Stolotermes* and *Porotermes* (Krishna et al. 2013). Their divergence from other termites dates back 115 Ma, i.e., prior to the final breakup of Pangaea (Bourguignon et al. 2015). As Gondwanan relicts, extant members of the genus *Porotermes* are endemic to Australia (*Porotermes adamsoni*) and the southernmost provinces of the Afrotropical (*Porotermes planiceps*) and Neotropical (*Porotermes quadricollis*) regions.

The gut flagellates of *P. adamsoni*, which was originally described as *Calotermes adamsoni* by Froggatt (1897) and later placed in the genus *Porotermes* by Desneux (1906), have been investigated by several authors. Grassi (1917) and Sutherland (1933) described eight species of parabasalids (*Joenina pulchella, Pseudotrypanosoma giganteum, Pseudotrypanosoma minimum, Spirotrichonympha grandis, Spirotrichonympha mirabilis, Spirotrichonymphella pudibunda, Trichonympha magna,* and an unspecified trichomonad); an additional species, *Microjoenia depressa*, was later added by Brugerolle (2001). The morphology and ultrastructure of several of these flagellates have been comprehensively studied (Brugerolle 1999, 2001; Brugerolle and Patterson 2001), and the SSU rRNA gene sequences of several species have been reported (Keeling et al. 1998; Izawa et al. 2017).

However, none of these studies ever mentioned the presence of oxymonad flagellates. To date, there is no record of oxymonads in any member of the Stolotermitidae, which leaves the impression that this basal termite family lacks oxymonad flagellates entirely. Here, we investigated the diversity of oxymonads in *P. adamsoni* and describe three novel, genus-level lineages of oxymonads. We present a detailed characterization of morphology and ultrastructure for two of these species and discuss possible implications of their phylogenetic position for the coevolutionary history of oxymonad flagellates and termites.

Results

We detected three morphotypes of oxymonad flagellates by light microscopy of the hindgut contents of *Porotermes adamsoni*. The smallest flagellate, *Termitimonas travisi* gen. nov. sp. nov., has a pointed anterior cell pole and resembles members of the genus *Monocercomonoides*. The second morphotype, *Oxynympha loricata* gen. nov. sp. nov., is slightly larger and possesses a long axostyle; it does not closely resemble any described species. The third morphotype resembled members of the genus *Saccinobaculus* and is very rare.

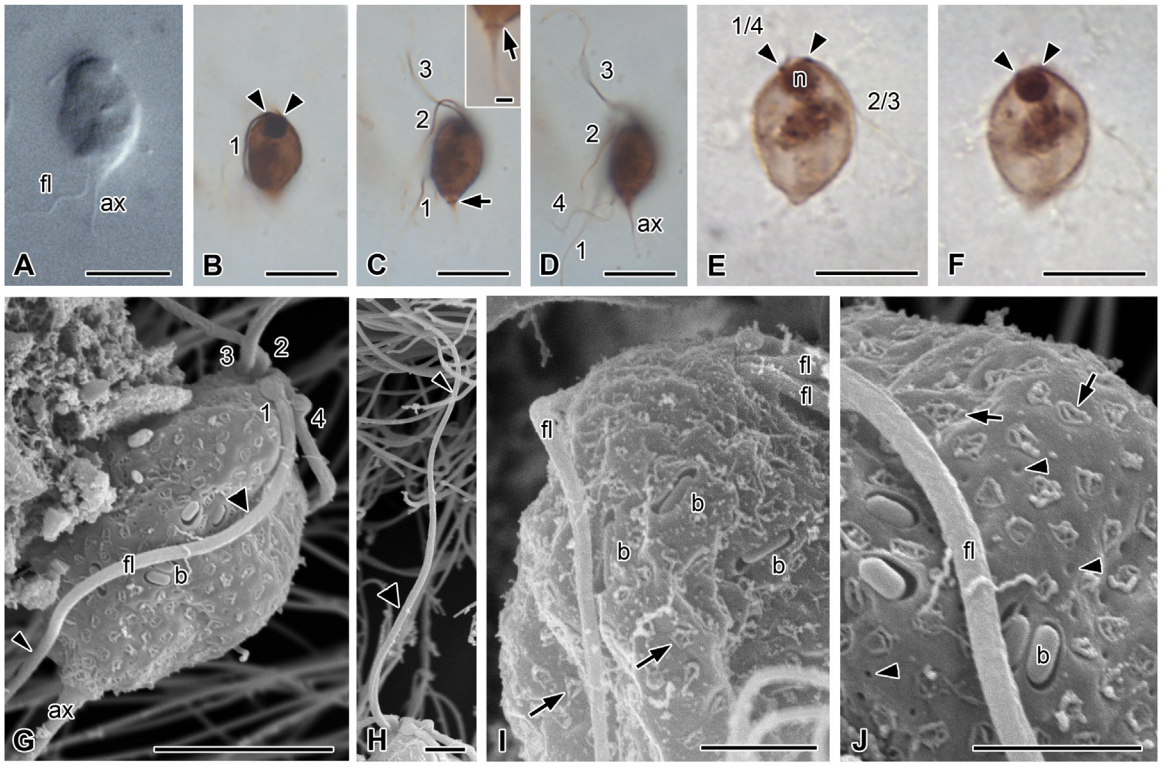

Figure 1. *Oxynympha loricata*, general cell morphology. Scale bars: A–F, 10 μm; C inset, 1 μm; G, 5 μm; H–J 2 μm. **A** Glutaraldehyde-fixed cell with posteriorly protruding axostyle (ax). fl, flagellum. **B–D** Different focal planes of a protargol-stained cell show all four flagella (1–4), which are robust and well stained. A darkly stained, globular nucleus lies close to the two pairs of basal bodies (arrowheads). The protruding axostyle has a darkly stained periaxostylar ring (arrow) at the point where it leaves the cell body proper (C, inset). **E, F** Another protargol-stained cell in two focal planes. Four flagella (1–4) arise from two pairs of basal bodies (arrowheads); n, nucleus. The periphery of the cell is conspicuously well stained. **G–J** Scanning electron micrographs. Proximally, the flagella are particularly thick (G, H wide arrowheads), compared to their more distal part (G, H narrow arrowheads). The surface is covered by scales (arrows) that seem to suffer during sample preparation; small holes probably represent the central funnel of intact scales (J arrowheads). Partially caved-in bacterial rods (b) occur. Axostyle protrudes posteriorly.

Morphological Characterization

Oxynympha loricata gen. nov. sp. nov.

Oxynympha loricata is the most common and second-smallest oxymonad of *P. adamsoni*. The cells have a slightly pointed posterior end, which gives them the appearance of an inverted egg. They have a length of 10.8 μm (9–12.5 μm, $n = 18$) and a width of 7.4 μm (5.6–9.4 μm, $n = 21$) (Fig. 1A–G). The long axostyle protrudes at the posterior cell pole by another 5–7 μm ($n = 9$) (Fig. 1A, D, G), which allows an easy distinction from the cells of *Termitimonas travisi*. At the point where the axostyle protrudes from the cell proper, a periaxostylar ring was evident in protargol-stained specimens (Fig. 1C and inset). Four flagella arise from two pairs of basal bodies (Fig. 1B–H). They appear unusually thick and stained intensively with protargol (Fig. 1C, D). SEM images revealed that the diameter of the flagella is larger in the proximal half (ca. 0.4 μm) than in the distal posterior half, which has a diameter typically found in other eukaryotes (0.2 μm) (Fig. 1G–I). The lengths of the flagella range from 22 to 30 μm (mean 27 μm; $n = 18$). The rounded nucleus is situated close to the anterior cell pole and has a mean diameter of 2.5 μm (2.0–3.2 μm, $n = 21$). Regions in the central and posterior regions of the cell stained dark (Fig. 1B, E, F). The periphery of the cell was strongly impregnated with protargol (Fig. 1C, E, F). The SEM images revealed the presence of loosely arranged ring-like surface structures (scales) (Fig. 1I, J), which occur on the cell proper but not on the flagella or the protruding axostyle. Furthermore, small holes were seen in the

smooth regions between the scales (Fig. 1J). The cell surface had elongate invaginations that contain rod-shaped bacteria of more or less uniform appearance (Fig. 1G, I, J).

TEM of ultra-thin sections showed that the anterior cell pole is mostly occupied by the large nucleus and various root structures arising from the basal body pairs (Figs 2A–E, 3 A). The nucleoplasm often contains coccoid bacteria (Figs 2A, 3 A). Anteriorly, the nucleus is indented by the preaxostyle, which connects the basal body pairs (Fig. 2A, D). The anterior plasma membrane is supported by a pelta; root 1 and a hook-like structure (ribbon b) arise close to basal body 1 (Fig. 2A, B). At the base of cross-sectioned basal bodies (distal from the axoneme of the flagellum) a typical cartwheel structure is present (Fig. 2C). Proximal to their origin at the anterior cell pole, the flagella have an irregular outline with a wide space between axoneme and plasma membrane (Fig. 2A, D and inset, D). In cross-sections of flagella, electron-dense triangles connect the doublets with the membrane (Fig. 2D). Longitudinal sections revealed that these triangles are long threads with a fine, regular striation (Fig. 2E). The proximal part of the recurrent flagellum is supported by microtubular root 1 (Fig. 2D inset, E). Axostyle microtubules arise in intimate contact to the preaxostyle (Fig. 2D). The axostyle consists of 5–6 layers of interconnected microtubules (Figs 2D, F, 3 C). The layers are more or less straight at the level of the nucleus (Fig. 2D) but are curved inwards by about one turn in the posterior part of the cell (Figs 2F, 3 C). The cytoplasm contains several morphotypes of prokaryotes. Some are thick-walled pleomorphic cells that are apparently not enclosed in vacuoles (Fig. 2D), and others are rod-shaped with a gram-negative cell wall; it was not always clear whether they were surrounded by a vacuole (Fig. 3A). Some internal bacteria looked degenerated (Fig. 3A). In addition, the external surface of each flagellate showed several rod-shaped prokaryotes deeply embedded in pouches formed by the plasma membrane (Fig. 3B). The posterior part of the cells also harbors large vacuoles with transparent and electron-dense, fine fibrillary regions (Fig. 3C), rough endoplasmic reticulum, and curls of free ribosomes (polysomes) (Figs 2F, 3 A).

Favorable sections of the cell periphery revealed a distinct ectoplasmic zone, which was much more electron-dense than the endoplasm (Fig. 3A, C). Vesicles with a dense inner coat occur close to the plasma membrane or even open to the surface (Fig. 3C and inset). The outside of the cell body is almost completely covered with scales, which sit in shallow indentations of the surface (Figs 2A, D, 3 A–D). The plasma membrane under the scales has a particularly prominent glycocalyx (Figs 2D, 3 A inset). In top view, the scales are rounded structures of about 0.5–0.6 μm (Figs 1I, J, 3 D). The scales consist of a circular rim (150–200 nm high) with a funnel-shaped lid (Figs 2A, D, 3 A and inset, 3B–D), whose borders are connected to the circular base by regularly spaced fibrillous material (Fig. 3A inset). In the center, the funnel-shaped lid contacts the plasma membrane via a short cylindrical part (Figs 2D, 3 A and inset, 3 B).

Termitimonas travisi gen. nov. sp. nov.

Termitimonas travisi is the smallest and second-most prevalent oxymonad in *P. adamsoni*. The cells have an average length of 7.7 μm (range 6–9.7 μm, $n = 11$) and an average width of 5.5 μm (range 3.8–6.5 μm, $n = 11$). The anterior cell pole is more or less pointed and lends the cells an ovoid-to-pyriform appearance (Fig. 4A–E). Four flagella arise anteriorly in two pairs (Fig. 4A, D, E). The length of the flagella ranges from 13 to 23 μm (mean 16 μm; $n = 5$); the preparations did not allow determination of the differences in length between individual flagella. Protargol-stained samples revealed two pairs of basal bodies (Fig. 4B), which are connected by a bowl-like preaxostyle (Fig. 4C) that is in contact with the nucleus. The nucleus is rounded, lies close to the anterior cell pole, and has a diameter of 2–2.5 μm (mean 2.3 μm, $n = 11$). The border of the nucleus often stained more strongly. The axostyle is a short, dark, longitudinal rod and does not protrude from the posterior cell pole (Fig. 4A–D). Other structures that were stained with protargol are a pelta, which supports the anterior cell pole (Fig. 4B), and root 1, which supports the recurrent flagellum (Fig. 4C). The cytoplasm and the cell border stained only faintly. Food vacuoles were not obvious. The SEM images clearly showed two pairs of flagella, one arising close to the anterior tip, and the other a bit shifted towards the posterior cell pole (Fig. 4D, E). The irregular surface is probably due to fixation artifacts.

Although we found only a single one of these tiny cells in the ultra-thin sections, TEM revealed other structural details. The plasma membrane, whose wrinkled appearance matches the irregular cell surface in the SEM images, is not covered by scales or ectobacteria. Typical oxymonadid structures occupy the anterior cell pole (Fig. 4F, G). A pelta supports the plasma membrane, and a narrow anterior microtubular root supports the pelta.

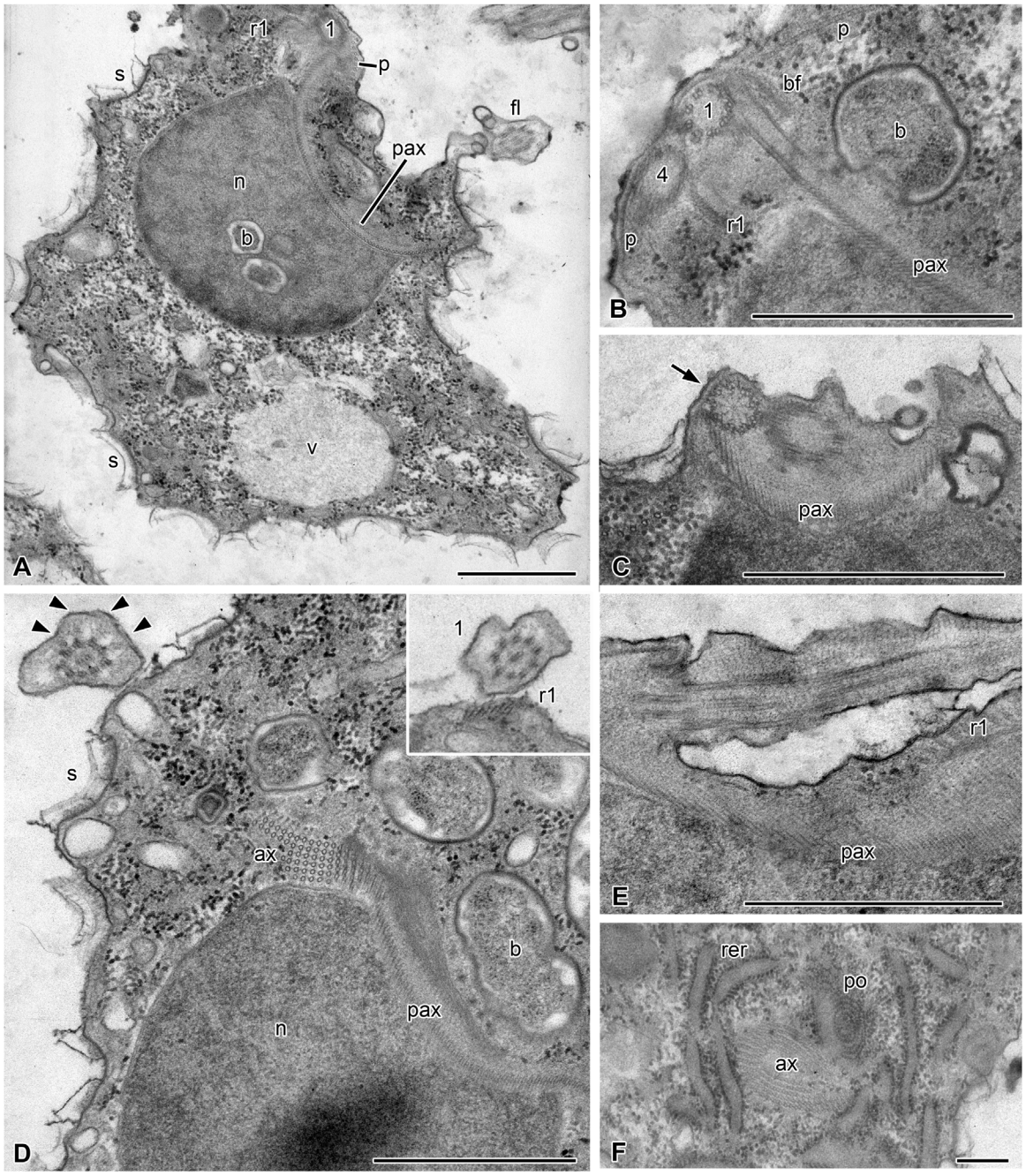

Figure 2. *Oxynympha loricata*, fine structure (TEM) of the anterior cell pole. Scale bars, 1 μm. **A, B** A curved preaxostyle (pax) is closely adjacent to the nucleus (n) and is in contact to basal body 1 (1). Root 1 (r1) arises between basal body 1 and 4, and the pelta microtubules (p) support the plasma membrane. b, bacteria; bf, b fiber; fl, flagellum; s, scale on surface; v, vacuole. **C** Cartwheel structure (arrow) in one of the basal bodies. **D** Cross-sectioned cell with microtubular layers of the axostyle (ax) arising from the preaxostyle. Cross-sectioned flagella show a wide lumen; some duplets of the axoneme are connected to the distant membrane by triangular structures. Attached part of the recurrent flagellum is supported by microtubular root 1 (r1; inset D). **E** Longitudinally sectioned flagellum. Fine regular striations connect the axoneme with the distant membrane. **F** Posterior to the nucleus, the sheets of the axostyle are curved in for one turn. Ribosomes are arranged as polysome curls (po) or rough endoplasmic reticulum (rer).

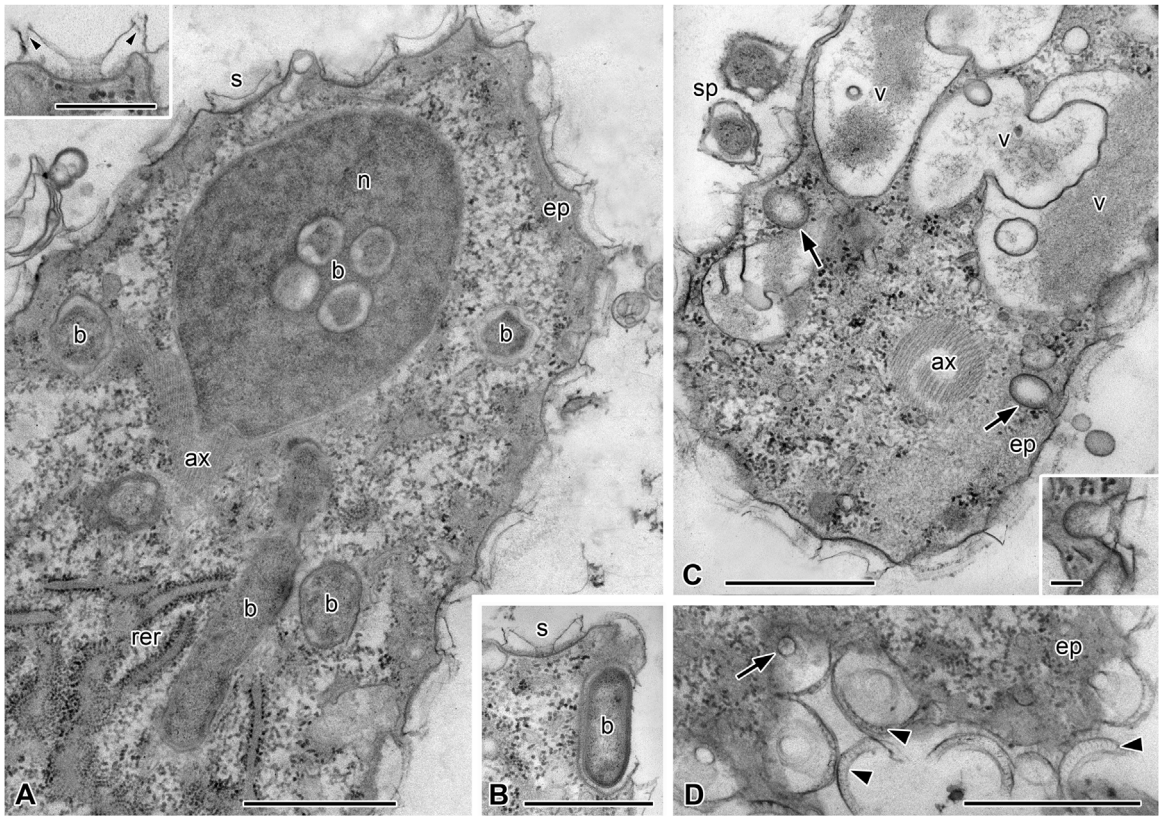

Figure 3. *Oxynympha loricata*, fine structure (TEM) of the posterior cell pole, surface, and cytoplasmic elements. Scale bars: 1 μm; inset A, 0.5 μm; inset C, 0.1 μm. **A** Median-sectioned cell with external layer of scales (s), dense ectoplasm layer (ep), nucleus (n) with coccoid bacteria (b), flat-cut axostyle (ax) posterior to the nucleus, light granular endoplasm containing bacteria and rough endoplasmic reticulum (rer). Inset: scale in higher magnification. A circular base is covered by a lid, which forms a deep funnel at its center. The lid is connected to the circular base by filaments (arrowheads). Plasma membrane under the lid possesses a thick glycocalyx. **B** Rod-like bacterium deeply sunken in indentation of the surface. **C** Cross-section through posterior cell pole. Large vacuoles (v) contain fine, fibrillary material. Small vacuoles with dense inner layer make contact to the plasma membrane (arrows). Inset: small opened vesicle under scale. sp, spirochaetes. **D** Grazing section of surface with horizontally sectioned scales. Outer circular base is connected to border of the lid by regularly spaced fibrils (arrowheads). Arrow points to central cylinder of funnel-shaped lid.

The preaxostyle connects the basal body pairs 1 + 4 with 2 + 3 (using the terminology of Simpson et al. 2002, which states that basal body 1 belongs to the recurrent flagellum and is associated with basal body 4, whereas the other pair consists of basal bodies 2 and 3). Root 1 and the axostyle both arise near basal body 1. The presence of root 1 confirmed the presence of a recurrent flagellum with partial attachment to the cell surface in addition to three freely moving flagella. A grazing section of the nucleus (Fig. 4F, G) showed superficial nuclear pores and endonuclear bacteria. The dense cytoplasm contains vacuoles with membranous content and cisterns of rough endoplasmic reticulum.

Saccinobaculus-like flagellate

The third morphotype is considerably larger than the other two. We observed only a few of these cells in live preparations (Fig. 5J–K). The cells constantly change their shape by rolling up into a ball and stretching their anterior pole, which suggests that they have a highly flexible and contractile axostyle, which is characteristic for members of the genus *Saccinobaculus*. We postponed the suggestion of a name and the species description until we have obtained enough material to investigate their ultrastructure in more detail.

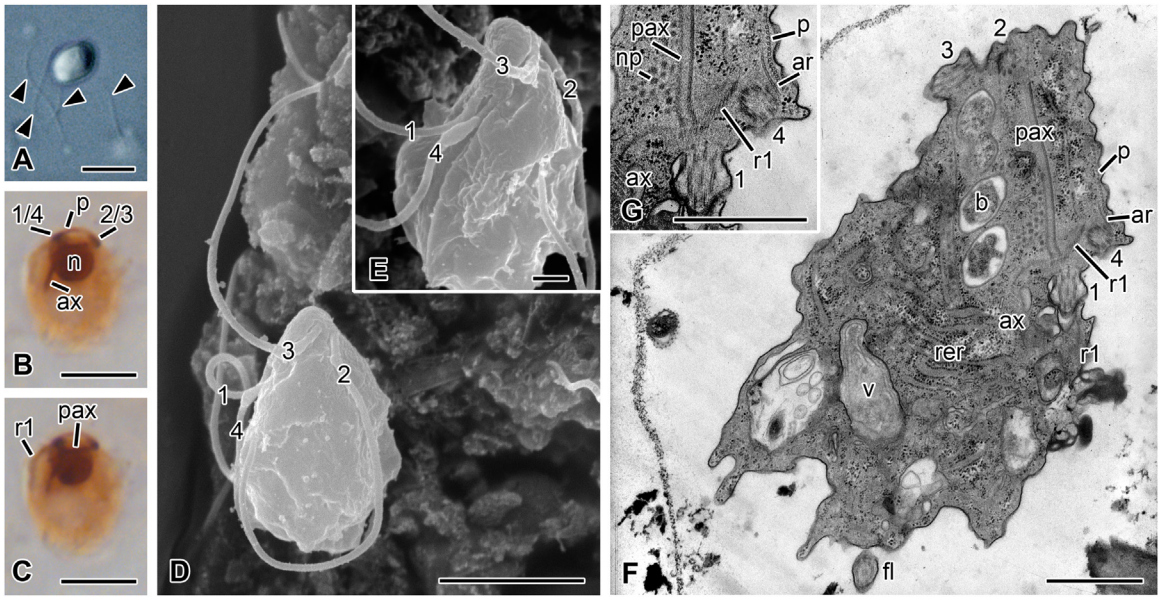

Figure 4. *Termitimonas travisi*. Scale bars: A–D, 5 μm; E–G, 1 μm. **A** Glutaraldehyde-fixed cell with four flagella (arrowheads). **B, C** Two slightly different focal planes of a protargol-stained cell, revealing two pairs of basal bodies (1 + 4 and 2 + 3) at the anterior cell pole, nucleus (n), axostyle (ax), preaxostyle (pax), and pelta (p). Root 1 (r1) supports the recurrent flagellum. **D, E,** Scanning electron micrographs of the same cell in slightly different views, showing the pointed anterior end of the cells and the two pairs of flagella (1 + 4, 2 + 3); the origin of pair 1 + 4 is shifted posteriorly. **F, G** Transmission electron micrographs showing the preaxostyle connecting basal bodies 1 + 4 and 2 + 3. The pelta arises near basal body 4 and is supported by the anterior root (ar). Root 1 will support the recurrent flagellum (1). Other structures: axostyle, bacteria (b), flagellum (fl), nuclear pores (np), rough endoplasmic reticulum (rer), vacuole (v).

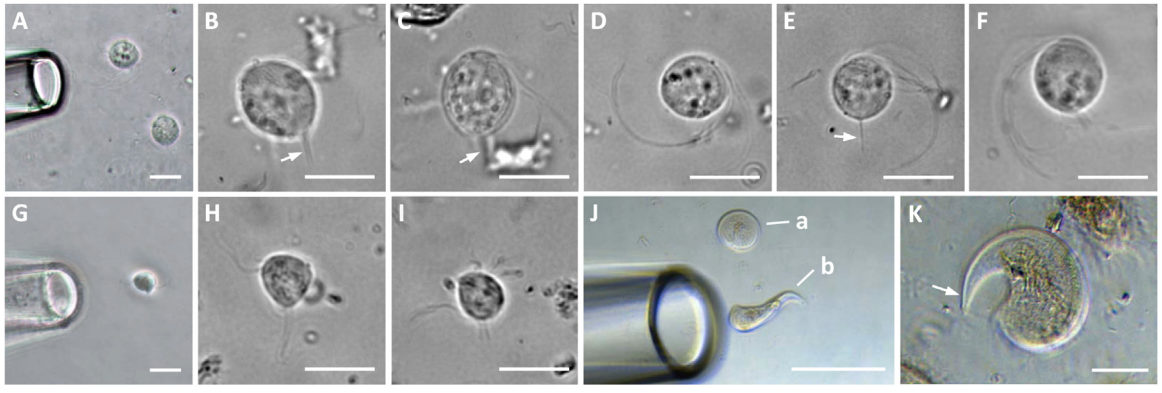

Figure 5. Capillary picking of individual cells of *Oxynympha loricata* (**A**), *Termitimonas travisi* (**G**), and the *Saccinobaculus*-like morphotype (**J**) for molecular identification. The cells of *O. loricata* (**B–F**) were distinguished from those of *T. travisi* (**H–I**) by their slightly larger size, their longer flagella, and their protruding axostyle (arrows). The *Saccinobaculus*-like morphotype was identified by its constantly changing shape (**J**, cells a and b) and the probing movement of its anterior cell pole (**K**, arrow). Phase-contrast micrographs of living cells. Scale bars: 10 μm, except J (50 μm).

Phylogenetic Analysis

The SSU rRNA gene sequences of oxymonads obtained from the hindgut of *P. adamsoni* fell into three distinct clades. They differed considerably with respect to amplicon length (1948, 2191, and 2012 bp, respectively) and showed a high sequence dissimilarity between members of the clades (16–20%). A thorough phylogenetic analysis based on a manually curated alignment of all

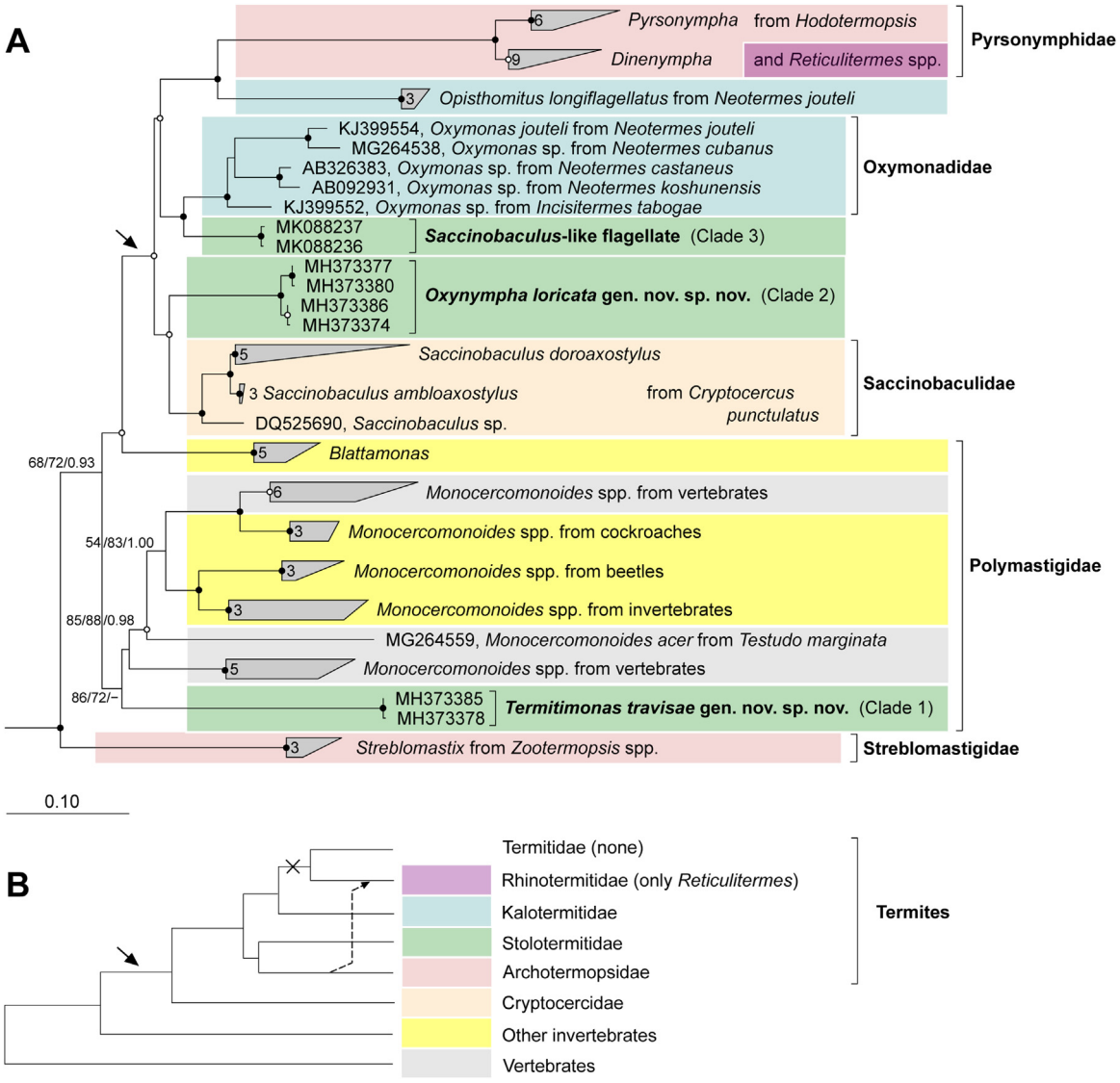

Figure 6. A Phylogenetic analysis of the SSU rRNA genes of Oxymonadida, showing the relationship of the three new species from *Porotermes adamsoni* obtained in the present study (in bold) to the oxymonads from other hosts. The arrow marks the clade whose members occur exclusively in termites and Cryptocercidae. The tree was reconstructed using maximum-likelihood analysis (PhyML), with members of Trimastigidae and Paratrimastigidae as outgroup. Tree topology was confirmed by IQ-TREE, RAxML, and Bayesian (Ba) analysis. Bullets summarize node support (aLRT support/ultrafast bootstrap support/posterior probabilities: ●, ≥95/99/1.00, ◯, ≥70/95/0.99); otherwise individual values are shown. The dash indicates a conflicting node in Ba. The background colors indicate the host range of the respective lineages. **B** Phylogenetic relationship of the host lineages with oxymonad symbionts (schematic). The arrow marks the ancestral acquisition and the cross the subsequent loss of the termite-specific clade of oxymonads (see A); the dashed line marks the proposed transfaunation event (see text). For more details, including accession numbers of all sequences and root information, see Supplementary Material Figure S2.

homologous gene sequences of the order Oxymonadida revealed that each clade represents a novel, deep-branching lineage of oxymonads (Fig. 6A).

Sequences of two clades were recovered already from a small clone library (20 clones). While Clade 1 (12 clones) consisted of a single phylotype (i.e., clones with a sequence similarity ≥99.7%),

Clade 2 (8 clones) comprised two phylotypes (4.3% dissimilarity). The third clade was detected only in a second, substantially larger clone library (93 clones), which yielded mostly sequences that belonged to Clade 1 (76 clones) and Clade 2 (15 clones). Sequences of Clade 3 were very rare (2 clones) and represented a single phylotype.

Clade 1 falls into the radiation of the family Polymastigidae. It forms a separate line of descent that is most closely related to members of the genus *Monocercomonoides*, which comprises several distinct lineages representing isolates from the intestinal tracts of either invertebrate or vertebrate hosts (Treitli et al. 2018). In all analyses, the genus *Blattamonas* formed a sister group to the higher taxa of Oxymonadida, and in trees inferred by Bayesian analysis, Clade 1 fell into a well-supported position basal to *Monocercomonoides* and *Blattamonas* (see Supplementary Material Fig. S2), which suggests that the family Polymastigidae may be paraphyletic.

The remaining higher taxa of Oxymonadida were monophyletic in all analyses, and the relationships between individual families were stable, irrespective of the method used for tree reconstruction. However, the sister position of Clade 2 to the family Saccinobaculidae is only weakly supported, which suggests that members of this lineage may represent an independent line of descent with family rank. By contrast, the sister-group position of Clade 3 to the genus *Oxymonas* was highly supported in all analyses.

Assignment of Morphotypes to Phylotypes

To assign the morphotypes to their respective phylotypes, we amplified the SSU rRNA from capillary-picked individual cells using nested PCR. Because the cells of *Oxynympha loricata* and *Termitimonas travisi* are very small and hard to distinguish in live preparations, we initially tested the procedure by amplifying the SSU rRNA genes from a mixed suspension of both morphotypes. Gel electrophoresis of the PCR products yielded two distinct bands (Supplementary Material Fig. S3) with the amplicon length predicted for the partial sequences of members of Clade 1 (1037 bp) and Clade 2 (1193 bp) generated with the internal primer pair. When both bands were excised and sequenced, they matched the corresponding phylotypes.

Then, we picked individual flagellates from these suspensions for single-cell PCR (Fig. 5). After some practice, it was possible to distinguish *O. loricata* by their slightly larger cells, with longer flagella and a protruding axostyle at the posterior cell pole. They rounded off when immersed in solution U, whereas those of *T. travisi* kept their irregular shape.

Only cells with the morphology of *O. loricata* yielded a PCR product. The partial sequences fell into Clade 2, confirming that *O. loricata* is the new lineage loosely affiliated with the Saccinobaculidae.

All attempts to amplify the SSU rRNA genes from single cells with the morphotype of *T. travisi* were unsuccessful. However, based on the presence of the phylotype of Clade 1 in the mixed suspension of both flagellates, we consider it safe to conclude that *T. travisi* represents the phylotype related to *Monocercomonoides*.

The third, *Saccinobaculus*-like species was easy to identify based on its size and characteristic motility. Although the cells were extremely rare, we were able to isolate an individual cell of this morphotype and successfully amplified its SSU rRNA gene. The sequence was virtually identical to those of Clade 3, which matches the low representation of this phylotype in the clone libraries. Based on these criteria, we tentatively assign the *Saccinobaculus*-like species to the new lineage of oxymonads that is sister to the Oxymonadidae.

Discussion

Oxymonads in termite guts were discovered almost 150 years ago (Leidy 1877). All extant genera had been established by the mid-20th century (Grassé 1952). More than 65 years after the last genus description from termites (*Sauromonas*), we found representatives of three new genus-level lineages of oxymonads in *Porotermes adamsoni*, two of which are described as new genera in the present study. This report establishes the presence of oxymonads in termites of the family Stolotermitidae and provides new insights into the internal phylogeny of Oxymonadida and their coevolution with lower termites.

Hidden Diversity of Oxymonads

The order Oxymonadida presently consists of the families Oxymonadidae, Polymastigidae, Pyrsonymphidae, Saccinobaculidae, and Streblomastigidae (Brugerolle and Lee 2000; Hampl 2016); the phylogenetically isolated members of the genus *Opisthomitus* might represent a sixth family-level lineage (Radek et al. 2014). The diversity and host distribution of extant species have been comprehensively reviewed by Yamin (1979) and Hampl

(2016). These species represent 11 genera that occur exclusively in termites, one genus (*Saccinobaculus*) from wood-roaches of the genus *Cryptocercus*, and three genera (*Brachymonas*, *Monocercomonoides,* and the recently described *Blattamonas*) that are found also in the guts of other insects and vertebrates, and even in anoxic habitats such as cesspits (Treitli et al. 2018).

Although the gut flagellates of *Porotermes adamsoni* have been studied by several authors (see Introduction), the presence of oxymonads has never been mentioned. It is likely that the earlier microscopy-based surveys overlooked the large *Saccinobaculus*-like morphotype because it is quite scarce, and the other two were probably neglected because of their tiny size. None of them were detected in previous molecular studies of *P. adamsoni* because the SSU rRNA genes were obtained from single cells of larger (parabasalid) flagellates and from clone libraries prepared with parabasalia-sized amplicons (Keeling et al. 1998). In another short-read library of total hindgut DNA generated with a general primer pair (Tai et al. 2015), the amplicons of oxymonad SSU rRNA genes probably remained undetected because they should have been much longer (*Oxynympha*, 1035 bp; *Termitimonas*, 878 bp; *Saccinobaculus*-like flagellate, 894 bp) and less abundant than those of the co-amplified parabasalids (590–600 bp).

Phylogeny of Oxymonads

In the eusocial termites and the subsocial Cryptocercidae, the gut flagellates are vertically transmitted to their progeny via proctodeal trophallaxis, i.e., the exchange of hindgut fluid among nestmates (Nalepa 2015). This behavior explains the high level of similarity of the flagellate assemblages within a termite genus and among termite family members (Kitade 2004; Tai et al. 2015; Yamin 1979). Although the distribution of flagellates strongly suggests a codiversification of the symbionts with their hosts, cocladogenesis has been documented only in the case of the parabasalid genus *Pseudotrichonympha* and termites of the family Rhinotermitidae (Noda et al. 2007).

There is ample evidence for a codistribution of different oxymonad genera and certain termite families (e.g., *Oxymonas*, *Opisthomitus* in Kalotermitidae; *Saccinobaculus* in Cryptocercidae; Fig. 6). All apical lineages of oxymonads (excluding Streblomastigidae and Polymastigidae) form a well-supported monophyletic clade, whose members are found exclusively in termites and cockroaches of the genus *Cryptocercus*. The sister-group position of Saccinobaculidae to the termite-specific families suggests that the entire clade was derived from an ancestral oxymonad that was acquired before termites and Cryptocercidae split more than 170 Ma ago (Bourguignon et al. 2015; see arrows in Fig. 6).

The absence of oxymonads from most Rhinotermitidae and all Termitidae, and the presence of two independent lines of descent in *Porotermes* (*Oxynympha* and the *Saccinobaculus*-like species) and *Neotermes* (*Oxymonas* and *Opisthomitus*) indicates that the vertical transmission of the oxymonad lineage was accompanied by at least one split and several independent losses of oxymonads during the evolution of lower termites. So far, the lack of information on the presence and molecular phylogeny of oxymonads in members of several basal termite families precludes a detailed hypothesis of the evolutionary history of the entire clade. The presence of hitherto undetected lineages of oxymonads in *P. adamsoni* underscores the necessity of a comprehensive investigation of oxymonads in termite guts, particularly in hitherto unstudied members of the basal termite families (Archotermopsidae, Hodotermitidae, Mastotermitidae).

In parabasalids, the evolutionary history of flagellates is complicated by the occasional horizontal transmission of flagellates between different host lineages (Kitade 2004; Radek et al. 2018). It has been proposed that the presence of closely related *Trichonympha* species in both *Hodotermopsis* and *Zootermopsis* species (Archotermopsidae) and in the genus *Reticulitermes* (Rhinotermitidae) is explained by a horizontal transfer (transfaunation) of flagellates to an ancestral *Reticulitermes* species, accompanied by the concomitant loss of other flagellates characteristic for rhinotermitids in the recipient (Kitade 2004; Radek et al. 2018). Such a transfaunation could also explain the conspicuous presence of oxymonads in all members of the genus *Reticulitermes*. Oxymonads are entirely absent from all other Rhinotermitidae, and the *Dinenympha* and *Pyrsonympha* species in *Reticulitermes* are closely related to their sister species in *Hodotermopsis* (Archotermopsidae), which strongly suggests that these pyrsonymphids were transferred during the same transfaunation event as the trichonymphids (see dashed line in Fig. 6B).

In contrast to the apical lineages of oxymonads, the phylogeny of the more basal lineages (Polymastigidae and Streblomastigidae) does not indicate a coevolutionary history with a particular host. While the members of several deep-branching lineages show a specificity for a particular host

group (*Blattamonas*, *Termitimonas*), members of the genus *Monocercomonoides* have apparently switched among a wide range of hosts (i.e., from invertebrates to vertebrates; Hampl 2016, Treitli et al. 2018). The apparent paraphyly of the Polymastigidae has to be treated with caution in view of the lack of sequence data for members of several genera (*Tubulimonoides*, *Paranotila, Polymastix*) and the uncharted diversity of polymastigids in both invertebrate and vertebrate hosts. Future studies will be greatly facilitated by the oxymonad-specific primers presented in this study and the growing alignment of SSU rRNA gene sequences of oxymonads.

Structural Characteristics

In contrast to the free-living members of Preaxostyla (*Trimastix, Paratrimastix*), oxymonads have a derived morphology probably evoked by their endobiotic lifestyle (Hampl 2016). Trimastigids are small and have a simple outer morphology with four flagella, but their internal cytoskeleton shows typical excavate features with many specific root structures (Simpson 2003; Simpson et al. 2000; Yubuki et al. 2016). Extant oxymonads have much more diverse cell forms and size ranges, but their typical excavate cytoskeleton has been reduced (Radek et al. 2014; Simpson et al. 2002). A problem in comparing structures of oxymonads is that different authors use different names for the same structures (Hampl 2016; Radek 1994; Simpson et al. 2002; Treitli et al. 2018; Yubuki and Leander 2013; Yubuki et al. 2016). We here used mainly the terminology of Simpson et al. (2002) in accordance with suggested homologies of the oxymonad cytoskeleton with that of typical excavate taxa. Since the identity of root 2 and 3 was used divergently, we instead preferred the more descriptive terms right root and anterior root (Simpson et al. 2002). The left root of excavates originates at basal body 1, corresponds to R1 in the universal scheme of eukaryotes (e.g., Heiss et al. 2013; Yubuki and Leander 2013), and is mostly called root 1 in oxymonads; therefore, we kept the latter name.

Termitimonas travisi gen. nov. sp. nov. forms a deep-branching lineage within the Polymastigidae, which is in agreement with its small cell size, the presence of four flagella, a pelta, a slender non-contractile axostyle, and the absence of an attachment organelle (Hampl 2016). It resembles members of the genus *Monocercomonoides* in cell size, the oval-to-pyriform shape of its body, the anterior position and arrangement of the two pairs of flagella, and the absence of scales (Brugerolle and Joyon 1973; Radek 1994; Simpson et al. 2002; Travis 1932). We do not have comprehensive data of the cytoskeletal elements of *O. loricata,* but typical structures also occurring in *Monocercomonoides* could be found: three freely moving flagella, one recurrent flagellum, axostyle, preaxostyle, pelta, root 1, and anterior root. However, as its deep-branching phylogenetic position clearly separates it from members of the genus *Monocercomonoides* (Fig. 6A), the creation of a new genus is required.

The morphological characteristics we observe in *T. travisi* exclude it from the polymastigid genera *Polymastix*, *Paranotila*, and *Tubulimonoides;* molecular data are missing. Members of the genus *Polymastix* occur in various insect taxa, including termites, but are densely covered by long ectobacteria (Grassé 1952). The cells of *Paranotila*, a monotypic genus described from the cockroach *Cryptocercus punctulatus,* are much larger (15–25 μm) than *T. travisi* and undergo sexual cycles during the molt of their host (Cleveland 1966). We did not observe any sexual cycles but did not specifically study the gut fauna of molting termites. The flagella in members of the genus *Tubulimonoides* (Krishnamurthy and Sultana 1976) are not arranged in two pairs but rather in a 3-plus-1 configuration; their classification among oxymonads is questionable *per se*.

Oxynympha loricata gen. nov. sp. nov. represents a novel, deep-branching lineage and a combination of morphological characters that is unique among oxymonads. Like the members of Polymastigidae, it is small, has four flagella, a pelta, a slender non-contractile axostyle, and no attachment organelle. However, its prominently protruding axostyle combined with the presence of a periaxostylar ring clearly distinguish it from most members of this family, the genus *Blattamonas* from cockroaches forming a notable exception (Treitli et al. 2018). Another distinguishing character is the shape of the flagella. While the flagella of polymastigids are uniform in diameter (0.2–0.25 μm), all four flagella of *O. loricata* are considerably thicker in their proximal part. Also in their internal morphology, they resemble the flagella of *Pyrsonympha* (Pyrsonymphidae), which have a wavy outline, a considerably thicker layer of cytoplasm around the axoneme, and show triangular connections between the microtubular duplets and the plasma membrane of the flagellum in cross-sections (Bloodgood et al. 1974; Brugerolle 1970; Grassé 1956; Hollande and Carruette-Valentin 1970).

A characteristic feature of many oxymonads is the presence of surface structures, which are

considered to stabilize the cells and serve as attachment devices for bacteria (Bloodgood et al. 1974; Rother et al. 1999; Smith and Arnott 1974). They are absent from Polymastigidae and most likely evolved several times in other oxymonads (Brugerolle 1970; Lavette 1973; Rother et al. 1999). The Oxymonadidae (*Oxymonas, Microrhopalodina*) have scale-like structures that consist of a cylindrical hollow basis covered by a circular lid, which is connected to the basis with fibrils (Rother et al. 1999). The scales of *O. loricata* have a similar structure but deviate in several details. The lid forms a central, cross-striated funnel that contacts the plasma membrane. While the plasma membrane of Oxymonadidae is deeply invaginated directly under the scales, the invaginations of *O. loricata* do not always correspond with the location of the scales. The surface structures of Pyrsonymphidae (*Pyrsonympha* and *Dinenympha*) have an entirely different morphology; they are composed of a straight stalk with prongs branching from the distal end (Smith and Arnott 1973). In our SEM samples, the scales of *O. loricata* appeared more variable in form and less densely distributed than the corresponding structures in the TEM samples. This is most likely due to their destruction during sample preparation. Most of the surface scales apparently collapsed to ring-like structures; only in some regions of the cell surface, the lids of the scales remained intact and connected to each other. Their central funnels appear as small holes with a smooth circumference.

In contrast to other oxymonads, such as *Microrhopalodina* and *Oxymonas* (Rother et al. 1999), there are no ectobacteria attached to the surface scales of *O. loricata*. However, both SEM and TEM showed a few rod-shaped bacteria deeply embedded into indentations of the cell surface between the scales, enabling a close contact between the cells. However, colonization is not very dense, and the plasma membrane of the flagellate does not show any specializations typical for cell contacts, such as an enhanced glycocalyx and electron-dense substances underneath the contact site (Radek et al. 1992, 1996; Radek and Tischendorf, 1999; Smith and Arnott 1974). In the cytoplasm, we occasionally observed small vacuoles with rod-shaped bacteria that appeared degraded, but it is not clear if they represent ectobacteria that were phagocytized by the flagellate. There are also larger vacuoles that do not contain remnants of bacterial cells walls but unstructured material of unknown nature. Similar vacuoles have been observed also other members of the Oxymonadida; it is possible that they are involved in scale production (Rother et al. 1999).

The rare *Saccinobaculus*-like species is unusual because it combines a highly contractile axostyle with a close affiliation to the family Oxymonadidae, whose axostyles are typically not very agile. Unfortunately, the number of individuals in the specimens of *P. adamsoni* investigated in this study was extremely low. For a detailed analysis of their ultrastructural features and their comparison with other oxymonad genera, more material is required. Since the larger termite gut flagellates may quickly deteriorate when the termite host is maintained under poor conditions, we hope that fixation of gut contents immediately after collection would preserve more cells of this species.

Taxonomic Summary

Oxynympha gen. nov.

Etymology: N.L. prefix *oxy-*, from Ancient Greek *oxús*, sharp, pointed; Gr. fem. n. *nymphe*, a beautiful maiden; figurative name for certain termite gut flagellates. N.L. fem. n. *Oxynympha*, a flagellate with a pointed shape.

Diagnosis: Small cells (9–13 μm long) without anterior rostellum. Proximal part of the four flagella about twice as thick as usual. Protruding axostyle with periaxostylar ring. Scales on surface.

Type species: *Oxynympha loricata*

Taxonomy: Preaxostyla, Oxymonadida; *incertae familiae*

Oxynympha loricata sp. nov.

Etymology: L. fem. n. *lōrīca*, a coat of mail, breastplate; L. fem. suff. *-ata*, provided with; N.L. fem. adj. *loricata*, harnessed, clad in mail, referring to the scales on the cell surface.

Diagnosis: Small, egg-shaped cells measuring 10.8 μm (9–12.5 μm) × 7.4 μm (5.6–9.4 μm). Well stainable ectoplasm zone; sometimes cytoplasmic and nuclear bacteria.

Type host: The hindgut of *Porotermes adamsoni* (Froggatt, 1897).

Type host locality: Fallen log near Lamington National Park, Queensland, Australia.

Type material: The holotype is a labelled cell on a protargol-stained microscopy slide deposited at the Biology Centre of the Upper Austrian Museum, J.-W.-Klein-Strasse 73, 4040 Linz, Austria under type number 2019/2. Holotype (label 1) and a paratype (label 2) have been outlined in black (see Supplementary Material Fig. S4).

Gene sequences: SSU rRNA gene accession numbers MH373374, MH373375, MH373377, MH373380, MH373386

ZooBank number: urn:lsid:zoobank.org:act:8A498B07-59EF-4B04-BBCD-DB98487C091F

Termitimonas gen. nov.

Etymology: L. n. *termes -itis*, a worm that eats wood, a termite. Gr. fem. n. *monas*, a unit, monad; here: a unicellular organism. N.L. fem. n. *Termitimonas*, a unicellular organism occurring in termites.

Diagnosis: Small cells (6–10 μm long) with four flagella, slender, non-contractile, and non-protruding axostyle, pelta, no attachment organelle, no surface scales.

Type species: *Termitimonas travisi*

Taxonomy: Preaxostyla, Oxymonadida, Polymastigidae

Termitimonas travisi sp. nov.

Etymology: N.L. gen. n. *travisi*, of Travis, named for Bernard V. Travis, American entomologist and parasitologist, who introduced the closely related genus *Monocercomonoides*.

Diagnosis: Cell body egg-to-pear-like, with a more or less pointed anterior cell pole and a rounded posterior cell pole. 7.7 μm in length (range 6–9.7 μm) and 5.5 μm in width (range 3.8–6.5 μm).

Type host: The hindgut of *Porotermes adamsoni* (Froggatt, 1897).

Type host locality: Fallen log near Lamington National Park, Queensland, Australia.

Type material: The holotype is a labelled cell on a protargol-stained microscopy slide deposited at the Biology Centre of the Upper Austrian Museum, J.-W.-Klein-Strasse 73, 4040 Linz, Austria under type number 2019/2. Holotype (left) and a paratype (right) have been outlined in red (see Supplementary Material Fig. S4).

Gene sequences: SSU rRNA gene accession numbers MH373373, MH373376, MH373378, MH373381, MH373385, MH373387.

ZooBank number: urn:lsid:zoobank.org:act:BC7CFD22-58AA-41EB-8676-85C6957BAC84

Methods

Termites: Specimens of *Porotermes adamsoni* (Froggatt) were collected from a decomposing log next to the access road to Lamington National Park, Queensland, Australia, in 2014 (Po218). Specimens used for the assignment of individual morphotypes to phylotypes were collected from a dead tree in a forest near East Kangaloon, New South Wales, Australia, in 2019 (Po515). Their identity was confirmed by COII gene sequence analysis (Inward et al. 2007); the Genbank accession numbers are MK736309 and MN306295. The deduced amino acid sequences were almost identical (>99% similarity) or identical to those of specimens previously identified as *P. adamsoni* (LC193947, Izawa et al. 2017; Supplementary Material Fig. S1).

Light microscopy: Termites were dissected with fine-tipped forceps. The hindgut paunch was opened either in 2.5% glutaraldehyde in 50 mM phosphate buffer, pH 7.0, for prolonged light microscopy observations, or in 0.6% NaCl and fixed with osmium vapors prior to protargol (silver proteinate) staining (procedure A; Foissner 1991). Protargol staining visualizes dictyosomes (parabasal bodies), basal bodies, flagella, nuclei, and axostyles. The slide mounts were observed with an Axiophot light microscope (Zeiss) equipped with differential interference contrast. Images were recorded with a MicroLive digital camera (Linkenheld, Oppenau, Germany; http://www.mikroskopie.de/). All measurements were taken from protargol-stained slides.

Electron microscopy: For scanning electron microscopy (SEM), the contents of the extracted hindguts were fixed in 2.5% glutaraldehyde, post-fixed in 1% OsO_4, dehydrated via increasing concentrations of ethanol, critical point dried, and sputtered with gold prior to examination with an environmental scanning electron microscope (FEI Quanta 200; FEI, Frankfurt/Main, Germany).

For transmission electron microscopy (TEM), samples were fixed in glutaraldehyde and OsO_4 solutions containing ruthenium red to enhance the visualization of the glycocalyx (Luft 1971). The samples were then washed, dehydrated, and embedded in Spurr's resin (Spurr 1969). Post-stained ultrathin sections were examined with a Philips EM 208 (FEI, Frankfurt/Main, Germany).

A more detailed description of the procedures can be found in Radek et al. (2018).

DNA extraction and amplification: The hindguts of five termites were pooled in an Eppendorf tube with 750 μl solution U (Trager 1934) and homogenized with a micro-pestle. DNA was extracted from the homogenate with the NucleoSpin kit for soil (Macherey-Nagel, Düren, Germany) following the manufacturer's instructions, except that the samples were not vortexed but instead subjected to bead beating in a FastPrep-24 (MP Biomedicals, Ilkirch, Germany) for 45 s at a velocity of 6.5 m/s to disrupt all microbial cells.

The SSU rRNA genes of oxymonad flagellates were amplified by PCR with a specific primer pair (OxyT21f, 5′-GCCAGTAGTCATATGCTTGTC-3′; Fla1484 r, 5′-CTTGTTACGACTTCTCCTTCC-3′). PCR started with a denaturing step at 94 °C for 3 min, followed by 30 cycles at 94 °C for 20 s, 58 °C for 20 s, and 72 °C for 50 s, and a final extension step at 72 °C for 7 min. PCR products were checked by gel electrophoresis (3% agarose) and cloned with the TOPO-TA cloning kit (Invitrogen).

Cloning, sequencing, and phylogenetic analysis: Inserts were amplified using M13 primers, checked for correct length by gel electrophoresis, and commercially sequenced using both internal primers (Oxy356f: 5′-AGGCGCGCAAATTACCCA-3′ and Oxy1057r: 5′-CCACCAACUAAGAACGACC-3′) and vector primers (T7 and M13 r) (GATC Biotech, Konstanz, Germany). Clones with a sequence similarity ≥99.7% were defined as one phylotype. All full-length sequences have been submitted to GenBank under accession numbers MH373370–MH373378, MH373380–MH373387, MK088236, MK088237.

The assembled sequences and all other oxymonadid sequences available in public databases were imported into the Silva SSURef database (Quast et al. 2013; version 106; http://www.arbsilva.de) using the ARB software package (Ludwig et al. 2004; version 6.0.6). After automatic alignment

of the full-length sequences against the prealigned reference sequences using *PT server* and *Fast Aligner* tool implemented in ARB, the alignment was manually refined, taking into account the secondary structure of the rRNA. After removing sites with >50% gaps, the alignment consisted of 1869 sites with unambiguously aligned base positions. After exclusion of highly variable positions (<50% identical bases), which decreases the likelihood of a site being homoplastic, the final alignment had 1655 positions, of which 766 were invariant and 747 were parsimony-informative sites.

Phylogenetic trees were reconstructed by maximum-likelihood analysis with *PhyML* v3.0 (Guindon et al. 2010) using the evolutionary model GTR + G + I suggested by *SMS* (Lefort et al. 2017). Tree topology was tested with *IQ-TREE* (Nguyen et al. 2015), *RaxML* (Stamatakis 2014), and Bayesian inference analysis (*MrBayes*, Ronquist et al. 2012; 1,000,000 generations, burn-in 0.25). Node support was assessed with the approximate likelihood ratio test (*aLRT*, Lemoine et al. 2018) and ultrafast bootstrap analysis (*UFBoot*, 1,000 replicates, Hoang et al. 2018).

When we tested the effects of automated alignment software (*MUSCLE*, Edgar 2004; *MAFFT*, (Katoh and Standley 2013) and/or masking algorithms (*GBlocks*, Talavera and Castresana 2007), the resulting trees showed the same the topology but node support was considerably lower. Also less stringent filtering of our alignment (inclusion of highly variable sites) decreased the bootstrap support and in some cases even changed the topology of the deep-branching nodes.

Identification of capillary-picked flagellates: Hindgut contents were carefully suspended in solution U (Trager 1934), and aliquots (10 μl) were transferred into the wells of a Teflon-coated microscope slide and inspected with an inverted phase-contrast microscope (Zeiss AxioVert A1, Jena, Germany) at 200- or 400-fold magnification. Individual flagellate cells were photographed with a CCD camera and collected by micropipetting using a Patchman NP 2 micromanipulator with CellTram vario (Eppendorf, Hamburg, Germany) with glass microcapillaries of 15 or 50 μm tip diameter, depending on cell size. Flagellate cells were transferred to PCR tubes in a droplet of solution U (ca. 2 μl), and their SSU rRNA genes were amplified using nested PCR with the primer pairs OxyT21f–Fla1484r and Oxy356f–Oxy1057r (see above) and commercially sequenced using the internal amplification primers. To ascertain the functionality of this procedure, we also used a mixed suspension of the two smaller morphotypes (ca. 20 cells each), checked the length of the amplicons by agarose gel electrophoresis, and verified their identity by excising and sequencing of the corresponding bands.

Funding

This research did not receive any specific grant from funding agencies in the public, commercial, or not-for-profit sectors.

Declarations of Interest

None.

Acknowledgements

We thank Regina Kollmann, Freie Universität Berlin, for technical assistance with electron microscopy.

Appendix A. Supplementary Data

Supplementary material related to this article can be found, in the online version, at doi:https://doi.org/10.1016/j.protis.2019.125683.

References

Adl SM, Bass D, Lane CE, Lukeš J, Schoch CL, Smirnov A, Agatha S, Berney C, Brown MW, Burki F, Cárdenas P, Čepička I, Chistyakova L, del Campo J, Dunthorn M, Edvardsen B, Eglit Y, Guillou L, Hampl V, Heiss A, Hoppenrath M, James TY, Karnkowska A, Karpov S, Kim E, Kolisko M, Kudryavtsev A, Lahr DJG, Lara E, Le Gall L, Lynn DH, Mann DG, Massana R, Mitchell EAD, Morrow C, Park JS, Pawlowski JW, Powell MJ, Richter DJ, Rueckert S, Shadwick L, Shimano S, Spiegel FW, Torruella G, Youssef N, Zlatogursky V, Zhang Q (2019) Revisions to the classification, nomenclature, and diversity of eukaryotes. J Eukaryot Microbiol **66**:4–119

Bloodgood RA, Miller KR, Fitzharris TP, Mcintosh JR (1974) The ultrastructure of *Pyrsonympha* and its associated microorganisms. J Morphol **143**:77–105

Bourguignon T, Lo N, Cameron SL, Šobotník J, Hayashi Y, Shigenobu S, Watanabe D, Roisin Y, Miura T, Evans TA (2015) The evolutionary history of termites as inferred from 66 mitochondrial genomes. Mol Biol Evol **32**:406–421

Brugerolle G (1970) Sur l'ultrastructure et la position systématique de *Pyrsonympha vertens* (Zooflagellata, Pyrsonymphina). Comp Rend Heb Séance Acad Sci, Paris **270**:966–969

Brugerolle G, Joyon L (1973) Ultrastructure du genre *Monocercomonoides* (Travis). Zooflagellata, Oxymonadida. Protistologica **9**:1–80

Brugerolle G (1991) Flagellar and cytoskeletal systems in amitochondrial flagellates: Archamoeba, Metamonada, and Parabasala. Protoplasma **164**:70–90

Brugerolle G (1999) Fine structure of *Pseudotrypanosoma giganteum* of *Porotermes*, a trichomonad with a contractile costa. Europ J Protistol **35**:121–128

Brugerolle G (2001) Morphological characters of spirotrichonymphids: *Microjoenia, Spirotrichonymphella* and *Spirotrichonympha* symbionts of the Australian termite *Porotermes grandis*. Europ J Protistol **37**:103–117

Brugerolle G, Lee JJ (2000) Oxymonadida. In Lee JJ, Leedale GF, Bradbury P (eds) An Illustrated Guide to the Protozoa **Vol. 2**. Society of Protozoologists, Lawrence, pp 1186–1195

Brugerolle G, Patterson DJ (2001) Ultrastructure of *Joenina pulchella* Grassi, 1917 (Protista, Parabasalia), a reassessment of evolutionary trends in the parabasalids, and a new order Cristamonadida for devescovinid, calonymphid and lophomonad flagellates. Org Divers Evol **1**:147–160

Brugerolle G, Radek R (2006) Symbiotic Protozoa of Termites. In König H, Varma A (eds) Soil Biology, Vol. 6, Intestinal Microorganisms of Soil Invertebrates. Springer, Berlin, Heidelberg, pp 243–269

Brune A (2014) Symbiotic digestion of lignocellulose in termite guts. Nat Rev Microbiol **12**:168–180

Brune A, Dietrich C (2015) The gut microbiota of termites: Digesting the diversity in the light of ecology and evolution. Annu Rev Microbiol **69**:145–166

Brune A, Ohkuma M (2011) Role of the Termite Gut Microbiota in Symbiotic Digestion. In Bignell DE, Roisin Y, Lo N (eds) Biology of Termites: A Modern Synthesis. Springer, Berlin, pp 439–475

Burki F (2016) Mitochondrial evolution: Going, going, gone. Curr Biol **26**:R410–R412

Cleveland LR (1966) Nuclear division without cytokinesis followed by fusion of pronuclei in *Paranotila lata* gen. et spec. nov. J Protozool **13**:132–136

Desneux J (1906) Variétés termitologiques. Ann Soc Entomol Belg **49**:336–360

Edgar RC (2004) MUSCLE: a multiple sequence alignment method with reduced time and space complexity. BMC Bioinformatics **5**:113

Foissner W (1991) Basic light and scanning electron microscopic methods for taxonomic studies of ciliated protozoa. Europ J Protistol **27**:313–330

Froggatt WW (1897) Australian Termitidae. Part II. Proc Linn Soc NSW **21**:510–552

Grassé PP (1952) Famille des Polymastigidae, ordre des Pyrsonymphines, ordre des Oxymonadines. In Grassé PP (ed) Traité de Zoologie **Vol. 1**. Masson, Paris, pp 780–823

Grassé PP (1956) L'ultrastructure de *Pyrsonympha vertens* (Zooflagellata Pyrsonymphina): les Flagellés et leur coadaptation avec le corps, l'axostyle contractile, le paraxostyle, le cytoplasme. Arch Biol **67**:595–611

Grassi B (1917) Flagellati viventi nei termiti. Mem R Accad Lincei, Ser **5(12)**:331–394

Guindon S, Dufayard JF, Lefort V, Anisimova M, Hordijk W, Gascuel O (2010) New algorithms and methods to estimate maximum-likelihood phylogenies: assessing the performance of PhyML 3. 0. Syst Biol **59**:307–321

Hampl V (2016) Preaxostyla. In Archibald JM, Simpson AGB, Slamovits CH (eds) Handbook of the Protists. Springer International Publishing, Switzerland, pp 1–36

Heiss AA, Keeling PJ (2006) The phylogenetic position of the oxymonad *Saccinobaculus* based on SSU rRNA. Protist **157**:335–344

Heiss AA, Walker G, Simpson AGB (2013) The flagellar apparatus of *Breviata anathema*, a eukaryote without a clear supergroup affinity. Europ J Protistol **49**:354–372

Hoang DT, Chernomor O, von Haeseler A, Minh BQ, Vinh LS (2018) UFBoot2: Improving the ultrafast bootstrap approximation. Mol Biol Evol **35**:518–522

Hollande MA, Carruette-Valentin J (1970) La lignée des Pyrsonymphines et les caractères infrastructuraux communs aux genres *Opisthomitus, Oxymonas, Saccinobaculus, Pyrsonympha* et *Streblomastix*. C R Acad Sci, Paris **270**:1587–1590

Honigberg BM (1970) Protozoa Associated with Termites and their Role in Digestion. In Krishna K, Weesner FM (eds) Biology of Termites. Academic Press, New York, pp 1–36

Inward DJG, Vogler AP, Eggleton P (2007) A comprehensive phylogenetic analysis of termites (Isoptera) illuminates key aspects of their evolutionary biology. Mol Phylogenet Evol **44**:953–967

Izawa K, Kuwahara H, Sugaya K, Lo N, Ohkuma M, Hongoh Y (2017) Discovery of ectosymbiotic *Endomicrobium* lineages associated with protists in the gut of stolotermitid termites. Environ Microbiol Rep **9**:411–418

Keeling PJ, Poulsen N, McFadden GI (1998) Phylogenetic diversity of parabasalian symbionts from termites, including the phylogenetic position of *Pseudotrypanosoma* and *Trichonympha*. J Eukaryot Microbiol **45**:643–650

Katoh K, Standley DM (2013) MAFFT Multiple sequence alignment software version 7: Improvements in performance and usability. Mol Biol Evol **30**:772–780

Kitade O (2004) Comparison of symbiotic flagellate faunae between termites and a wood-feeding cockroach of the genus *Cryptocercus*. Microbes Environ **19**:215–220

Krishna K, Grimaldi DA, Krishna V, Engel MS (2013) Treatise on the Isoptera of the World. Vol. 2. Basal Families. Bull Am Mus Nat Hist **377**:205–621

Krishnamurthy R, Sultana T (1976) *Tubulimonoides gryllotalpae* n. g., n. sp. (Mastigophora: Oxymonadida) from the cricket in India. Proc Ind Acad Sci, Sect B Oct **84**:137–140

Lavette A (1973) Sur la cuticule d'un Flagellé termiticole, *Pyrsonympha vertens*: glycocalyx et pinocytose. C R Acad Sci Paris, Ser D **276**:981–983

Lefort V, Longueville JE, Gascuel O (2017) SMS: smart model selection in PhyML. Mol Biol Evol **34**:2422–2424

Leidy J (1877) On intestinal parasites of *Termes flavipes*. Proc Nat Acad Sci, Phil **29**:146–149

Lemoine F, Domelevo Entfellner JB, Wilkinson E, Correia D, Dávila Felipe M, De Oliveira T, Gascuel O (2018) Renewing Felsenstein's phylogenetic bootstrap in the era of big data. Nature **556**:452–456

Ludwig W, Strunk O, Westram R, Richter L, Meier H, Yadhukumar A, Buchner A, Lai T, Steppi S, Jacob G, Förster W, Brettske I, Gerber S, Ginhart AW, Gross O, Grumann S, Hermann S, Jost R, König A, Liss T, Lüßmann R, May

M, Nonhoff B, Reichel B, Strehlow R, Stamatakis A, Stuckmann N, Vilbig A, Lenke M, Ludwig T, Bode A, Schleifer K-H (2004) ARB: A software environment for sequence data. Nucleic Acids Res **32**:1363–1371

Luft JH (1971) Ruthenium red and violet. I. Chemistry, purification, methods of use for electron microscopy and mechanism of action. Anat Rec **171**:347–368

Moriya S, Dacks JB, Takagi A, Noda S, Ohkuma M, Doolittle WF, Kudo T (2003) Molecular phylogeny of three oxymonad genera: *Pyrsonympha, Dinenympha* and *Oxymonas*. J Eukaryot Microbiol **50**:190–197

Moriya S, Ohkuma M, Kudo T (1998) Phylogenetic position of symbiotic protist *Dinenympha exilis* in the hindgut of the termite *Reticulitermes speratus* inferred from the protein phylogeny of elongation factor 1α. Gene **210**:221–227

Nalepa CA (2015) Origin of termite eusociality: trophallaxis integrates the social, nutritional, and microbial environments. Ecol Entomol **40**:323–335

Nguyen LT, Schmidt HA, von Haeseler A, Minh BQ (2015) IQ-TREE: A fast and effective stochastic algorithm for estimating maximum likelihood phylogenies. Mol Biol Evol **32**:268–274

Noda S, Kitade O, Inoue T, Kawai M, Kanuka M, Hiroshima K, Hongoh Y, Constantino R, Uys V, Zhong J, Kudo T, Ohkuma M (2007) Cospeciation in the triplex symbiosis of termite gut protists (*Pseudotrichonympha* spp.), their hosts, and their bacterial endosymbionts. Mol Ecol **16**:1257–1266

Quast C, Pruesse E, Yilmaz P, Gerken J, Schweer T, Yarza P, Peplies J, Glöckner FO (2013) The SILVA ribosomal RNA gene database project: Improved data processing and web-based tools. Nucleic Acids Res **41**:590–596

Radek R (1994) *Monocercomonoides termitis* n. sp., an oxymonad from the lower termite *Kalotermes sinaicus*. Arch Protistenkd **144**:373–382

Radek R, Hausmann K, Breunig A (1992) Ectobiotic and endocytobiotic bacteria associated with the termite flagellate *Joenia annectens*. Acta Protozool **31**:93–107

Radek R, Rösel J, Hausmann K (1996) Light and electron microscopic study of the bacterial adhesion to termite flagellates applying lectin cytochemistry. Protoplasma **193**:105–122

Radek R, Tischendorf G (1999) Bacterial adhesion to different termite flagellates: ultrastructural and functional evidence for distinct molecular attachment modes. Protoplasma **207**:43–53

Radek R, Strassert JFH, Krüger J, Meuser K, Scheffrahn RH, Brune A (2014) Phylogeny and ultrastructure of *Oxymonas jouteli*, a rostellum-free species, and *Opisthomitus longiflagellatus* sp. nov., oxymonadid flagellates from the gut of *Neotermes jouteli*. Protist **165**:384–399

Radek R, Meuser K, Strassert JFH, Arslan O, Teßmer A, Šobotník J, Sillam-Dussès D, Nink RA, Brune A (2018) Exclusive gut flagellates of Serritermitidae suggest a major transfaunation event in lower termites: Description of *Heliconympha glossotermitis* gen. nov. spec. nov. J Eukaryot Microbiol **65**:77–92

Ronquist F, Teslenko M, van der Mark P, Ayres DL, Darling A, Höhna S, Larget B, Liu L, Suchard MA, Huelsenbeck JP (2012) MrBayes 3. 2: Efficient Bayesian phylogenetic inference and model choice across a large model space. Syst Biol **61**:539–542

Rother A, Radek R, Hausmann K (1999) Characterization of surface structures covering termite flagellates of the family Oxymonadidae and ultrastructure of two oxymonad species, *Microrhopalodina multinucleata* and *Oxymonas* sp. Europ J Protistol **35**:1–16

Simpson AGB (2003) Cytoskeletal organization, phylogenetic affinities and systematics in the contentious taxon Excavata (Eukaryota). Int J Syst Evol Microbiol **53**:1759–1777

Simpson AGB, Bernard C, Patterson DJ (2000) The ultrastructure of *Trimastix marina* Kent, 1880 (Eukaryota), an excavate flagellate. Europ J Protistol **36**:229–251

Simpson AGB, Radek R, Dacks JB, O'Kelly CJ (2002) How oxymonads lost their groove: An ultrastructural comparison of *Monocercomonoides* and excavate taxa. J Eukaryot Microbiol **49**:239–248

Smith HE, Arnott HJ (1973) Scales associated with the external surface of *Pyrsonympha vertens*. Trans Am Microsc Soc **92**:670–677

Smith HE, Arnott HJ (1974) Epi- and endobiotic bacteria associated with *Pyrsonympha vertens*, a symbiotic protozoon of the termite *Reticulitermes flavipes*. Trans Am Microsc Soc **93**:180–194

Spurr AR (1969) A low viscosity epoxy resin embedding medium for electron microscopy. J Ultrastruct Res **26**:31–43

Stamatakis A (2014) RAxML version 8: a tool for phylogenetic analysis and post-analysis of large phylogenies. Bioinformatics **30**:1312–1313

Stingl U, Brune A (2003) Phylogenetic diversity and whole-cell hybridization of oxymonad flagellates from the hindgut of the wood-feeding lower termite *Reticulitermes flavipes*. Protist **154**:147–155

Sutherland JL (1933) Protozoa from Australian termites. Quart J Microsc Sci **76**:145–173

Tai V, James ER, Nalepa CA, Scheffrahn RH, Perlman SJ, Keeling PJ (2015) The role of host phylogeny varies in shaping microbial diversity in the hindguts of lower termites. Appl Environ Microbiol **81**:1059–1070

Talavera G, Castresana J (2007) Improvement of phylogenies after removing divergent and ambiguously aligned blocks from protein sequence alignments. Syst Biol **56**:564–577

Trager W (1934) The cultivation of a cellulose-digesting flagellate, *Trichomonas termopsidis*, and of certain other termite protozoa. Biol Bull **66**:182–190

Travis BV (1932) A discussion of synonymy in the nomenclature of certain insect flagellates, with the description of a new flagellate from the larvae of *Ligyrodes relictus* Say (Coleoptera-Scarabaeidae). Iowa State Coll J Sci **6**:317–323

Treitli SC, Kotyk M, Yubuki N, Jirounková E, Vlasáková J, Smejkalová P, Šípek P, Čepička I, Hampl V (2018) Molecular and morphological diversity of the oxymonad genera *Monocercomonoides* and *Blattamonas* gen. nov. Protist **169**:744–783

Yamin MA (1979) Flagellates of the orders Trichomonadida Kirby, Oxymonadida Grassé, and Hypermastigida Grassi &

Foà reported from lower termites (Isoptera families Mastotermitidae, Kalotermitidae, Hodotermitidae, Termopsidae, Rhinotermitidae, and Serritermitidae) and from the wood-feeding roach *Cryptocercus* (Dictyoptera: Cryptocercidae). Sociobiology **4**:1–119

Yubuki N, Leander BS (2013) Evolution of microtubule organizing centers across the tree of eukaryotes. Plant J **75**:230–244

Yubuki N, Čepička I, Leander BS (2016) Evolution of the microtubular cytoskeleton (flagellar apparatus) in parasitic protists. Mol Biochem Parasitol **209**:26–34